[1]D. Kuse and H. R. Zeller, Phys. Rev. Lett. 27, 1060 (1971).
[2]A. H. Bloch, R. B. Weisman, and C. M. Varma, Phys. Rev. Lett. 28, 753 (1972).
[3]L. K. Monteith, L. F. Ballard, C. G. Pitts, B. K. Klein, L. M. Slifkin, and J. P. Collman, Solid State Commun. 6, 301 (1968).
[4]L. V. Interrante and F. P. Bundy, J. Chem. Soc. D 10, 584 (1970), and Inorg. Chem. 10, 1169 (1971).
[5]J. Collman, J. Polym. Sci., Part C 29, 133 (1970).
[6]M. Atoji, J. W. Richardson, and R. E. Rundle, J. Amer. Chem. Soc. 79, 3017 (1957).
[7]J. R. Miller, J. Chem. Soc., London 1965, 713; P. Day, A. F. Orchard, A. J. Thomson, and R. J. P. Williams, J. Chem. Phys. 42, 1973 (1965).
[8]J. P. Collman, L. F. Ballard, L. K. Monteith, C. G. Pitt, and L. Slifkin, in *International Symposium on Decomposition of Organometallic Compounds to Refractory Ceramics, Metals, and Metal Alloys*, edited by K. S. Mazdiyasni (Univ. of Dayton Research Institute, Dayton, Ohio, 1968), pp. 269–283.
[9]P. S. Gomm, T. W. Thomas, and A. E. Underhill, J. Chem. Soc. A 1971, 2154.
[10]L. V. Interrante and R. P. Messmer, Inorg. Chem. 10, 1174 (1971).
[11]L. V. Interrante, J. Chem. Soc., Chem Commun. 6, 302 (1972).
[12]C. N. R. Rao and S. N. Bhat, Inorg. Nucl. Chem. Lett. 5, 531 (1969).
[13]E. Fishman and L. V. Interrante, Inorg. Chem. 11, 1722 (1972).
[14]B. A. Scott and F. Mehran, to be published.
[15]B. Bleaney, K. D. Bowers, and M. H. L. Pryce, Proc. Roy. Soc., Ser. A 228, 166 (1955).
[16]T. Krigas and M. T. Rogers, J. Chem. Phys. 55, 3035 (1971).
[17]M. Tinkham, Proc. Roy. Soc., Ser. A 236, 535 (1956).
[18]J. Owen and K. W. H. Stevens, Nature (London) 171, 836 (1953).
[19]P. W. Anderson, J. Phys. Soc. Jap. 9, 316 (1954); G. Feher, Phys. Rev. 114, 1219 (1959).
[20]D. J. Lepine, Phys. Rev. B 2, 2429 (1970).
[21]C. K. Jorgensen, Mol. Phys. 2, 309 (1959).
[22]B. Bleaney, Proc. Phys. Soc., London, Sect. A 63, 407 (1950).
[23]We have also obtained samples of high-conductivity ($\sim 10^{-2}\ \Omega^{-1}\ \mathrm{cm}^{-1}$) and low-conductivity ($\sim 10^{-4}$–$10^{-5}\ \Omega^{-1}\ \mathrm{cm}^{-1}$) MGS crystals from Dr. L. V. Interrante of the General Electric Research and Development Laboratory. We find strong signals in his high-conductivity crystals, with EPR parameters *completely identical* to our values. Practically no signals could be discerned in his low-conductivity MGS. The crystals measured were typically ~ 0.3 mm thick by ~ 1 mm long.

Surface-State Transitions of Silicon in Electron Energy-Loss Spectra

J. E. Rowe and H. Ibach*
Bell Laboratories, Murray Hill, New Jersey 07974
(Received 11 January 1973; revised manuscript received 12 June 1973)

Surface-state transitions on ordered silicon (100)2×1 and (111)7×7 surfaces have been observed by electron energy-loss spectroscopy. The surface transitions were identified by comparing the clean ordered surfaces with clean disordered surfaces, and with disordered surfaces due to submonolayer quantities of absorbed oxygen. Three transitions are observed corresponding to surface states near the top, near the middle, and at the bottom of the valence band. These surface-state transitions are stronger on the (111)-7×7 surface than on the (100)2×1 surface.

Characteristic excitations of solids can be observed in the energy distributions, $N(E)$, of inelastically scattered electrons. For most nearly free-electron materials such as aluminum, energy-loss spectroscopy (ELS) reveals bulk plasmon oscillations at a loss energy $E_L=\hbar(4\pi ne^2/m)^{1/2}\hbar\omega_p$ and surface plasmon oscillations at a smaller energy $\hbar\omega_s=\hbar\omega_p/\sqrt{2}$.[1,2] Silicon is expected to be such a free-electron–like crystal since the interband transitions occur at low energies in the range 3–6 eV, and previous measurements have reported both bulk plasmon and surface plasmon oscillations.[3-5] In this paper we show that atomically clean silicon surfaces exhibit surface-state transitions in addition to the bulk interband transitions and plasmon transitions previously observed.[3-5] The surface states were identified by adsorption of oxygen or by Ar^+ ion bombardment. In addition to surface states near the top of the valence band (previously observed in photoemission[6,7]), these measurements give evidence of surface states near the bottom of the valence band similar to those predicted.[8]

Single crystals of n-type silicon ($n\approx 5\times10^{17}$ cm^{-3}) were oriented, polished, and cut into 10

$\times 20 \times 0.2$-mm^3 slabs using standard techniques and mounted in an ultrahigh-vacuum chamber which had a base pressure $\sim 5 \times 10^{-11}$ Torr. The surface composition was monitored using Auger electron spectroscopy (AES) with a minimum detectability estimated at 0.005 monolayers corresponding to a noise level 2000 times smaller than the main silicon LVV Auger peak at 92 eV.[9] This low surface impurity level could be achieved after several hours of sputter etching with a 5-μA/cm^2 beam of 1000-eV Ar^+ ions.

The crystalline order of the surface was studied by low-energy electron diffraction (LEED). In agreement with previous LEED studies,[10,11] a minimum annealing temperature of ~ 700°C was required to remove the lattice disorder caused by Ar^+ ion bombardment. In most experiments involving lengthy Ar^+ bombardment, a higher temperature of ~ 900°C was used to produce a sharp LEED pattern with a ~ 10-min anneal.

Measurements of characteristic ELS in the range $0 \leq E_L \leq 20$ eV were performed using the coaxial cylindrical electron analyzer used for AES.[9] The coaxial electron gun gave satisfactory operating performance for primary electron energies E_p as low as 10 eV. However, the ELS data presented in this paper were taken with $E_p = 100$ eV. Similar results were obtained at other energies with the general feature that the surface-state transitions were stronger relative to the bulk transitions as E_p decreased.

The ELS results presented as the negative second derivative of the electron energy distribution[12] at $E_p = 100$ eV are shown for Si(100) in Fig. 1 and for Si(111) in Fig. 2. Three different surface conditions were studied which resulted in the three ELS curves a, b, and c in Figs. 1 and 2. The bulk features[13,14] found in these curves were the E_1 interband transition near 3.5 eV, the E_2 interband transition near 5 eV, the bulk plasmon oscillation near 17 eV, and the surface plasmon oscillation near 11 eV, somewhat lower than the $\hbar\omega_p/\sqrt{2}$ value of 12.1 eV. Note that in the second-derivative spectrum the bulk plasmon loss appears as a nearly symmetrical peak. This indicates that $-d^2N/dE^2$ provides a faithful representation of the loss spectrum. In addition, there are surface-state transitions characteristic of the clean ordered surfaces near 2, 8, and 15 eV, labeled S_1, S_2, and S_3, respectively. The lowest-energy transition S_1 appears to be stronger on the ion-bombarded disordered surface than on

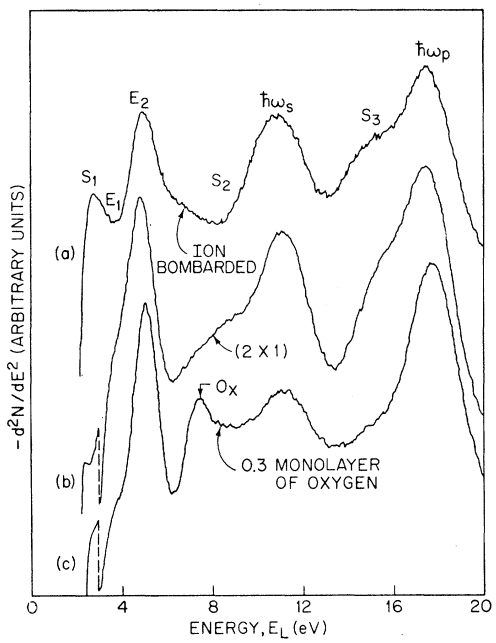

FIG. 1. Second-derivative electron energy-loss spectra at $E_p = 100$ eV for silicon (100) surfaces which are (trace a) clean but disordered following Ar^+-ion bombardment, (trace b) clean and ordered resulting in a sharp 2×1 LEED pattern, and (trace c) after partial formation of a disordered surface oxide at $\theta = 0.3$ monolayers of oxygen coverage.

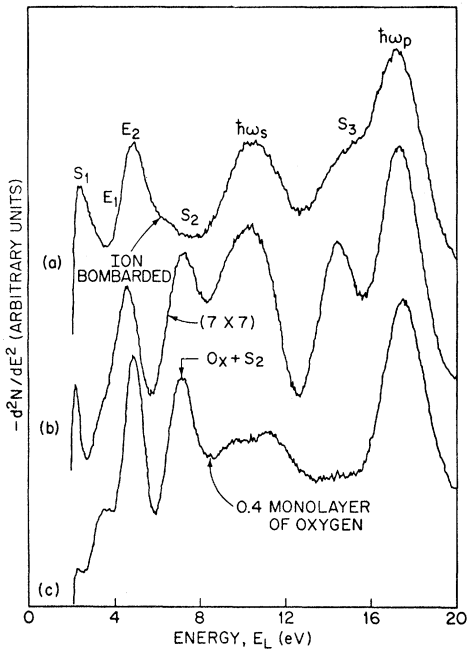

FIG. 2. Second-derivative electron energy-loss spectra at $E_p = 100$ eV for silicon (111) surfaces after (trace a) Ar^+-ion bombardment, (trace b) annealed to produce a sharp 7×7 LEED pattern, and (trace c) at $\theta = 0.4$ monolayers of a surface oxide.

TABLE I. Surface transition energies (eV).

	S_1	S_2	S_3	O_x
		Si(100)		
a, Ion bombarded	2.8±0.4	•••	14.7±0.6	•••
b, 2×1	1.7±0.4	8.4±0.8	14.7±0.8	•••
c, Oxide, $\theta=0.3$	•••	•••	•••	7.2±0.4
		Si(111)		
a, Ion bombarded	2.4±0.4	•••	14.4±0.6	•••
b, 7×7	2.0±0.4	7.4±0.4	14.5±0.4	•••
c, Oxide, $\theta=0.4$	•••	•••	•••	7.2±0.4

the clean ordered 2×1 and 7×7 structures, and has essentially disappeared with adsorption of 0.3–0.4 monolayer of oxygen.[15]

The transition S_2 appears as a shoulder below the surface plasmon transition for the (100)2×1 surface, but is a well-defined peak for the (111)-7×7 surface. This transition occurs only on the clean ordered surfaces. The transition S_3 occurs on all clean surfaces studied. It is a broad shoulder below the bulk plasmon transition on both (100) clean surfaces and on the Ar^+ bombarded (111) surface, but is a strong peak on the (111)7×7 surface. In addition to the intrinsic surface-state transitions, we observed a transition O_x at 7.2±0.4 eV due to the formation of a surface oxide. This transition is more easily observed on the (100) surface than on the (111) surface where it overlaps the S_2 transition.

A summary of the surface-related transition energies is given in Table I. These correspond to the peaks and shoulders shown in Figs. 1 and 2 and are probably somewhat larger than one would obtain in an optical-absorption measurement. For bulk transitions optical absorption measures $\mathrm{Im}\epsilon(\omega)$, while ELS measures $\mathrm{Im}[1/\epsilon(\omega)]$, where $\epsilon(\omega)$ is the complex dielectric function. This results in 0.3–0.8-eV shifts to higher energy in ELS compared with optical-absorption results. Similar shifts are expected for surface transitions.

Because of its low energy the S_1 transition can be associated with initial states due to dangling bonds at an energy near the top of the valence band. The dangling-bond states may exist in more than one layer for the ion-bombarded surface and should therefore have the greatest strength for this surface condition. Oxygen adsorption tends to saturate the dangling bonds (which are energetically unstable) as does the lattice reconstruction to some extent. Thus one expects the dangling-bond effects to decrease in strength from curves *a* to *c* in Figs. 1 and 2.

The transition S_2 is present only on the ordered 2×1 and 7×7 surfaces. Thus it appears to be associated with surface states below the upper *p*-like part of the valence band and is formed by reconstruction or by relaxation of the lattice. The S_2 transition could also involve higher unoccupied surface states with the same initial state as S_1. The transition S_3 is narrowest on the (111)7×7 surface, and from its large transition energy, 14.5±0.4 eV, one can estimate that the initial state would be at least 9.5 eV below the top of the valence band by assuming that the final-state energy lies between the vacuum level and the Fermi level. This gives strong evidence for surface states associated with the bottom of the bulk valence band. A detailed understanding of these transitions requires a better understanding of surface lattice reconstruction than has been previously achieved. However, in the absence of any knowledge of matrix-element effects and available final states, an approximate model for the surface density of states can be obtained by assuming a single final state. This is shown in Fig. 3 only for the (111) surface since the transitions S_2 and S_3 are much narrower on the (111)-7×7 surface than on the other surfaces studied. The solid curve in Fig. 3 is the calculated bulk density of states for silicon[16] and is similar to several other theoretical calculations as well as to so called "optical density of states" measured by photoemission[17] and soft-x-ray emission spectroscopies.[18] The dashed vertical lines are obtained from the transition energies given in Table I by assuming a single final state and by placing the initial state for S_1 at the top of the valence band. This results in surface-state energy positions corresponding to low densities of bulk states. Of course, the model assuming only one final state is probably not correct, but even when one allows for a relatively large uncertain-

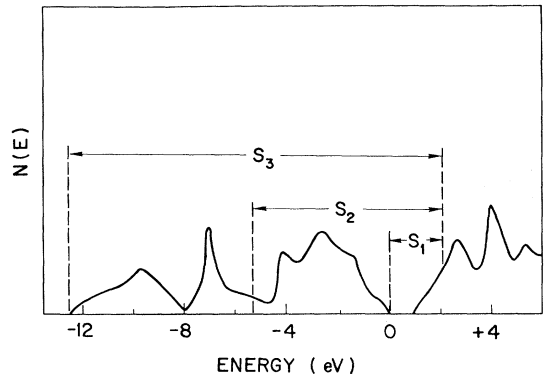

FIG. 3. Schematic model of surface-state ELS transitions for Si(111)7×7. Solid curve, Kane's theoretical bulk density of states. Dashed vertical lines, approximate surface-state positions, assuming only one final state. Symmetry considerations based on the calculations of Ref. 8 indicate that there should be two final states.

ty of ± 1 eV in the positions of initial states shown in Fig. 3, there is still very little overlap between the strong peaks in the bulk density of states and the surface-state density.

The qualitative picture of the surface-state density shown in Fig. 3 is remarkably similar to a recent theory by Appelbaum and Hamann[8] of the surface-state density for a relaxed (111)-1×1 surface. They find extra surface states below the top of the valence band which occur as a result of an increase in bond strength (over the bulk value) for bonds between the first and second layers. Although some details of their calculation are not expected to apply to the (111)-7×7 surface or to the (100)2×1 surface, the occurrence of additional surface states due to changes in the bonding of the first and second layers seems to be a general result. A more detailed understanding of the relationship between surface states and surface lattice structure is possible by combining the ELS measurements with ultraviolet photoemission measurements and by studying additional surface structures. Such experiments are currently in progress and will be reported at a later time.

The authors would like to acknowledge a number of helpful discussions with J. A. Appelbaum, H. D. Hagstrum, D. R. Hamann, J. C. Phillips, J. C. Tracy, and J. A. Van Vechten. The technical assistance of S. B. Christman in taking some of the data and of E. E. Chaban in constructing some of the apparatus is also greatly appreciated.

---

*On leave of absence from 2. Phys. Institut, Technische Hochschule, Aachen, Germany.

[1]R. H. Ritchie, Phys. Rev. 106, 874 (1957).

[2]E. A. Stern and R. A. Ferrell, Phys. Rev. 120, 130 (1960).

[3]H. Raether, in *Springer Tracts in Modern Physics, Ergebnisse der exakten Naturwissenschaften,* edited by G. Höhler (Springer, Berlin, 1965), Vol. 38, p. 84.

[4]M. Erbudak and T. E. Fischer, Phys. Rev. Lett. 29, 732 (1972).

[5]E. Bauer, Z. Phys. 224, 19 (1969).

[6]D. E. Eastman and W. D. Grobman, Phys. Rev. Lett. 28, 1378 (1972).

[7]L. F. Wagner and W. E. Spicer, Phys. Rev. Lett. 28, 1381 (1972).

[8]J. A. Appelbaum and D. R. Hamann, following Letter [Phys. Rev. Lett. 30, 106 (1973)].

[9]The AES spectrometer was a cylindrical mirror analyzer model 10-234G with a normal-incidence coaxial electron gun manufactured by Physical Electronics Industries, Edina, Minn.

[10]J. J. Lander, G. W. Gobeli, and J. Morrison, J. Appl. Phys. 34, 2298 (1963).

[11]R. E. Schlier and H. E. Farnsworth, J. Chem. Phys. 30, 917 (1959); F. Jona, IBM J. Res. Develop. 9, 375 (1965).

[12]The negative derivative was chosen rather than the first derivative used in AES, since peaks in $-d^2N/dE^2$ appear at essentially the same energies as peaks in $N(E)$.

[13]H. R. Philipp and H. Ehrenreich, Phys. Rev. 129, 1550 (1963).

[14]L. R. Saravia and D. Brust, Phys. Rev. 171, 916 (1968).

[15]The oxygen coverage was determined by AES (H. Ibach and J. E. Rowe, to be published).

[16]E. O. Kane, Phys. Rev. 146, 558 (1966).

[17]W. D. Grobman and D. E. Eastman, Phys. Rev. Lett. 29, 1508 (1972); L. Ley, S. Kowalczyk, R. Pollak, and D. A. Shirley, Phys. Rev. Lett. 29, 1088 (1972).

[18]G. Wiech, in *Soft X-Ray Band Spectra,* edited by D. J. Fabian (Academic, New York, 1968), p. 59.